Proteins mediating different DNA topologies block RNAP elongation with different efficiency

Yue Lu[1], Gustavo Borias[1], Zsuzsanna Voros[1], Christine Henderson[1], Keith Shearwin[2]

David Dunlap[1], Laura Finzi[1]

[1]Physics Department, Emory University, Atlanta, GA, USA

[2] Department of Molecular and Biomedical Science, University of Adelaide, Adelaide, Australia

Abstract

Many DNA-binding proteins induce topological structures such as loops or wraps through binding to two or more sites along the DNA. Such topologies may regulate transcription initiation and may also be roadblocks for elongating RNA polymerase (RNAP). Remarkably, a lac repressor protein bound to a weak binding site (O2) does not obstruct RNAP in vitro but becomes an effective roadblock when securing a loop of 400 bp between two widely separated binding sites. To investigate whether topological structures mediated by proteins bound to closely spaced binding sites and interacting cooperatively also represent roadblocks, we compared the effect of the λ CI and 186 CI repressors on RNAP elongation. Dimers of λ CI can bind to two sets of adjacent sites separated by hundreds of bp and form a DNA loop via the interaction between their C-terminal domains. The 186 CI protein can form a wheel of seven dimers around which specific DNA binding sequences can wrap. Atomic force microscopy (AFM) was used to image transcription elongation complexes of DNA templates that contained binding sites for either the λ or 186 CI repressor. While RNAP elongated past λ CI on unlooped DNA, as well as past 186 CI-wrapped DNA, it did not pass the λ CI-mediated loop. These results may indicate that protein-mediated loops with widely separated binding sites more effectively block transcription than a wrapped topology with multiple, closely spaced binding sites.

Introduction

Genomic DNA is decorated with proteins which have various, and often multiple, functions. Proteins may compact DNA[1, 2], protect it from the damaging effect of external agents[3, 4], mediate long-range interactions implicated, for example, in the management of DNA superhelicity[5, 6], repair[7-9], or transcription regulation[10, 11]. Whatever their function(s) might be, these proteins are in the path of elongating RNA polymerases and may act as roadblocks, interfering with RNA polymerase processivity. The mechanisms by which RNA polymerase might surpass such roadblocks are poorly understood. Single-molecule approaches are ideally suited to dissect such mechanisms and previous studies have focused on RNA polymerase

disrupting nucleosomes, which are not found in bacteria[12-15]. However, the histone proteins which form nucleosomes interact with the DNA non-specifically, and are substrates for post-translational modifications that regulate chromatin remodeling and the recruitment of accessory factors that regulate transcription[16, 17]. In contrast, transcription factors (TFs) from organisms spanning all kingdoms recognize specific sites on DNA[18, 19] to shape the genome and regulate various genomic functions and may or may not undergo chemical modifications regulated by complex pathways. Very often these TFs recognize not one but multiple specific sequences to which they bind with different affinities and cooperatively [20, 21]. These cooperative interactions determine ubiquitous (and often hierarchical) topological structures such as DNA looping, or wrapping, the role of which has not been directly investigated in earlier studies on elongation through roadblocks either *in vivo* or *in vitro*.

Recently, it was shown that the lac repressor (LacI) protein is an effective roadblock in vitro for an incoming RNAP on a linear template when bound to strong operators, such as Oid or O1 (Kd = 0.13 nM and 0.6 nM, respectively) but not if bound to the weak O2 (Kd = 2.7 nM) [22]. However, subsequent studies revealed that LacI turns into a strong roadblock even when bound to O2, if engaged in loop closure[23, 24]. Lac repressor forms a homo-tetramer with two DNA binding domains. Thus, just one LacI can bind two operators simultaneously, causing the looping out of the intervening DNA[25, 26]. However, many other repressors and, transcription factors in general, cause looping via the interaction between proteins bound at distant sites[27, 28]. In yet a different case of cooperativity, proteins may form structures that wrap DNA. Here, we extended the study of topological roadblocks to transcription elongation to include two proteins that capture these common patterns of DNA-protein interactions with packaging and regulatory functions: the λ and the 186 CI repressors[29, 30]. After infection of the bacterium *E. coli* by the λ bacteriophage, the λ CI repressor is responsible for lysogeny maintenance and, under the appropriate circumstances, switch to lysis[31, 32]. The repressor binds as a dimer to each of three adjacent operators (OL1, OL2 and OL3) in one region of the bacteriophage DNA and to three (OR1, OR2 and OR3) in another[33] (Figure S1). While the N-terminal domain of the dimer binds to an operator, the C-terminal can interact with the C-terminal of an adjacently bound dimer, in a dumb-bell configuration, and with the C-terminal of a juxtaposed dimer[34, 35]. These are the type of protein-protein interactions that stabilize the closure of a DNA loop between the OL and OR regions[36-41]. Thus, we used the λ CI repressor as a paradigm for DNA-looping proteins necessitating protein-protein cooperativity. The 186 CI repressor has a similar role to that of λ CI in regulating the lysogeny versus lysis switch once the 186 bacteriophage has infected *E. coli*[42, 43]. However, dimers of 186 CI oligomerize to form a wheel-shaped heptamer around which DNA wraps dynamically as three of the seven dimers bind to three strong (Kd = 30 nM)[42], specific binding sites at pR, favoring the weaker binding of the other dimers in the wheel to adjacent non-specific sequences which include pL[30, 44, 45] (Figure S1). Two more specific binding sites, FL and FR, are found, each on either side of pR. When pL is not wrapped on the wheel, the latter may bridge pR and either FR or FL[46]. Here we used the pR/pL and FR sequences along with the 186 CI repressor as a paradigm of DNA-wrapping proteins.

To compare the ability of these different forms of protein-DNA binding to block an elongating RNAP, we ran transcription assays on DNA templates where the λ CI-mediated

loop may form, as well as on templates where the 186 CI may mediate either a DNA wrap or loop. We analyzed snapshots of transcription elongation complexes (TECs) imaged with the atomic force microscope (AFM) similarly to what had recently been done for the lac repressor protein[23] and found that, while the λ CI protein was not a roadblock to an incoming RNAP on linear DNA, it was when mediating a loop. Given the previous study on the blocking capability of the LacI protein in the loop-securing configuration[23], it seems that proteins securing DNA loops may often be significant roadblocks. However, loops between pR/pL and FR were not observed and indeed they were estimated to be rare in a previous study[47], and this study shows that the DNA-wrapped 186 CI protein was not a roadblock either.

Comparison of the roadblocking ability of a DNA looping protein with a DNA wrapping protein indicates that proteins mediating loops may be stronger roadblocks than proteins that wrap DNA. Since proteins, such as CTCF in eukaryotes, or HU in prokaryotes are also defining and separating large loops of transcriptionally active domains (TADs)[48-50], it is intriguing to think that proteins which secure loops may be intrinsically stronger barriers for transcription. This may highlight a special functional motif for the looped topology in genomes.

Material and Methods

DNA constructs for scanning force microscopy

The DNA templates used for AFM measurements of the effect of λ CI on RNAP transcription were 1523 bp in length and were produced by PCR using plasmid template pUC18-LambdaLoop400 (Genbank format files in supplementary information), with two unlabeled primers (Table S1); and purified using a GeneJet PCR Cleanup kit (Thermo Scientific, Waltham, MA). The templates contained the T7A1 promoter, the OL and OR regions separated by 448 bp and a λt1 terminator (Figure 1, top).

The DNA templates used for AFM measurements of the effect of 186 CI on RNAP transcription were 1510 bp in length and were produced by PCR using plasmid template pT7A1_pRpL-FR (Genbank format files in supplementary information), using an unlabeled forward primer and a biotin-labeled reverse primer (Table S1). PCR products were purified using a GeneJet PCR Cleanup kit (Thermo Scientific, Waltham, MA). The fragments contained the T7A1 promoter, the three 186 pR binding sites, the pL site, the FR site, the λt1 terminator and a biotin, allowing labeling the end furthest from the promoter (Figure 1, top).

Sample preparation for scanning force microscopy

A 10 μL droplet of 0.01 μg/ml of poly-L-ornithine (1 kDa Mw, Sigma-Aldrich, St. Louis, MO) was deposited onto freshly cleaved mica and incubated for 2 min. The poly-L-ornithine-coated mica was then rinsed drop-wise with 600 μl of high-performance liquid chromatography-grade water and dried with compressed air. Nucleo-protein complexes of RNA polymerase/λ CI, or 186 CI, bound at the promoter (PC)/CI binding sites were produced by incubating 1 nM of DNA with 150 nM λ CI, or 250/300/500 nM 186 CI and 0.1 μM streptavidin, and RNA polymerase holoenzyme (New England Biolabs, Ipswitch, MA)

diluted in transcription buffer (TXB: 20 mM Tris-glutamate (pH 8.0), 10 mM magnesium-glutamate, 50 mM potassium-glutamate, 1 mM DTT) to a final concentration of 6 U/ml for 30 min at 37 degrees Celsius. To initiate transcription, the reaction mixture was spiked with 1 mM NTPs to give a final NTP concentration at 100 μM, and incubated at 37 degrees Celsius for 2 min. Then, 250 mM EDTA in TXB were added to give a final concentration of 20 mM EDTA and incubated at 37 degrees Celsius for 30 s to terminate transcription. 5 μl of this final mixture were deposited on the poly-L-ornithine-coated mica and incubated for 2 min. This droplet was rinsed with 600 μl of high-performance liquid chromatography-grade water and dried gently with compressed air[23, 46, 51].

Scanning force microscopy and DNA/protein data measurement

Images were acquired with a NanoScope MultiMode VIII AFM microscope (Bruker Nano Surfaces, Santa Barbara, CA, USA) operating in soft tapping mode, or scanasyst mode, using cantilevers with 2 nm nominal tip radius. Areas of 4×4 μm^2 were scanned at a rate of 0.5 Hz with a resolution of 2048×2048 pixels. After filtering the images to remove scan line offsets and tilt/bow, DNA/protein molecules were measured with NanoScope Analysis. The length measurement function was used to get the contour length of DNA length and establish the position of particle binding; lengths were then normalized by setting them all to 1523 bp, or 1510 bp. The Particle Analysis function was used to obtain the protein molecule diameter, height and volume.

Results

λ CI mediating a loop rather than bound on unlooped DNA interferes with RNA polymerase elongation.

The composition, conformation and elongation stage of transcription complexes were easily identifiable in AFM micrographs. To understand how RNAP navigates the λ CI - DNA nucleoprotein complex, we used scanning force microscopy. The DNA molecule contained two regions of three operators for the λ CI protein. The OL region, located 294 bp downstream of the T7A1 promoter contained the OL1, OL2 and OL3 operators. The OR region, separated from OL by 448 bp was located 673 bp away from the terminator and also contained three operators: OR1, OR2, OR3 [Figure 1, top]. Because of the relative binding affinity of the operators for λ CI, OR1=OR2=OL1=OL2>OL3>OR3[52, 53], and the pairwise nature of the interaction of adjacent λ CI dimers, on a linear DNA molecule[34], there might be three λ CI dimers at OL and only two at OR[41, 54]. However, loops are thermodynamically stable when closed by six λ CI dimers both in vitro [37]and in vivo (ref 50) Transcription was activated and halted by adding NTPs and EDTA, respectively (Materials and Methods). An aliquot of the sample was then immediately deposited on poly-L-ornithine-coated mica, incubated, rinsed, and dried for imaging.

As expected, the λ CI protein-induced a DNA loop on the path of an elongating RNAP. Snapshots of transcription complexes were collected and scored according to the position of

RNAP along the template and the unlooped/looped conformation of the DNA-λ CI nucleoprotein complex. The molecular weight of RNAP is several hundred kDa, much larger than that of λ CI (MW_{dimer} ~ 40 kDa), which makes them easily distinguishable [Figure 1, right panel]. Although some of the unlooped DNA molecules had λ CI bound to either the OL, or the OR region, these were easily discernable by their different distance from the closest end: ~300 bp for OL and ~600 bp for OR. In any case, most of the DNA molecules had both OR and OL regions occupied by λ CI. The left and right panels of Figure 1 describe the classification method followed for the analysis of the AFM images and a representative gallery of images, respectively. The unlooped complexes were classified according to the position of RNAP before OL, between OL and OR, or after OR. The looped complexes were scored according to their position before, inside, or after the λ CI-mediated loop.

Unlooped λ CI complex cannot stop elongation. Upon addition of NTPs, RNAP was found at all stages of elongation in unlooped complexes, as gathered both from the RNAP location along the template and the presence of nascent RNA. This suggests that RNAP is able to bypass the λ CI obstacle. In addition, most complexes showed λ CI bound to both operator regions [Figure 1, top row] suggesting that λ CI promptly rebinds its operators after having been dislodged by RNAP.

The surviving fraction of elongation complexes as a function of distance from the promoter along the DNA molecule is shown in Figure 2A. The frequency distribution of the λ CI position along the DNA template is described by the orange and green histogram bars which indicate that λ CI binds OL/OR specifically. The red data points represent RNAP progress without NTPs. In this condition, RNAP is only found at the promoter (Figure S2, top left). The pink curve represents the progress of RNAP with NTP but without λ CI (Figure S2, right). The blue curve represents transcription progress in the presence of λ CI. Elongating RNAP seems to proceed unimpeded from promoter to terminator regardless of the presence of λ CI. If λ CI were a strong obstacle for the transcription elongation complex (TEC), the blue curve in Figure 2A would display a steep drop in the probability of finding RNAP at the OL region.

λ CI mediating a DNA loop is an effective roadblock for RNAP elongation. In all the templates where λ CI was mediating a DNA loop, TECs were found before the loop, none were found either within or after the loop (Figure 1 bottom row). This indicates that RNAP may not be able to bypass the λ CI protein when this is engaged in closing the loop. Indeed, the surviving fraction of elongation complexes as a function of distance from the promoter along looped DNA molecules (Figure 2B) shows that no RNAP is found past the OL region. In this panel too, the frequency distribution of the λ CI position along the DNA template is described by the orange and green histogram bars which indicate that λ CI binds OL/OR specifically, the red curve represents RNAP progress without NTP and shows that all points are near the promoter (Figure S2, bottom left). The blue curve, instead, represents RNAP progress on DNA looped by a λ CI oligomer. The curve decreases steeply to 0 in correspondence of the first λ CI peak (OL region). This observation supports the idea that RNAP polymerase cannot bypass the looped DNA-λ CI complex and that the strength of the

λ CI roadblock changes considerably, depending if the protein is engaged, or not, in closing a DNA loop.

186 CI is not an effective obstacle to transcription.

186 CI and RNA polymerase can be distinguished by height. Micrographs of TECs in the presence of the 186 CI repressor were acquired to score the location of RNA polymerase and the 186 CI obstacle along DNA templates that contained two 186 CI-binding regions. The first binding region contained the three 186 strong pR sites adjacent to the weaker pL site. Together these sites can wrap around the 186 heptamer to form a stable wheel-like structure. The second region, ~370bp away from the promoter, contained the 186 FR site which has a lower affinity than pR for 186 CI. Thus, the DNA construct used here has the pR-pL region located 326 bp downstream of the T7A1 promoter and 372 bp upstream of the FR site. A λt1 terminator was located 617 bp downstream of FR and the end of the template closest to it was labeled with a biotin on the 5' strand [Figure 3, top]. The 186 CI (500 nM), streptavidin and RNAP were added to a DNA solution at the same time and transcription was activated and stopped as described in Materials and Methods by addition of NTPs and EDTA, respectively. Measurements were conducted in the same manner as those with the λ CI repressor, but this time, a streptavidin molecule bound to the biotin label made the terminator end of the DNA template immediately recognizable (Figures 3 and S3A, purple arrow). The majority of the DNA molecules were found to have an RNAP [Figure 3, Figure S3A, green arrow] bound at the promoter and 186 CI [Figure 3, Figure S3A, orange arrow] bound at the pR/pL, as well as at the FR site. Both 186 CI and RNAP appear roundish in AFM images and have similar size between 15 - 25 nm. While RNA polymerase is characterized by an average 4.5 nm height, 186 CI's average height is only 2 nm [Figure S3B]. Thus, 186 CI and RNAP can be distinguished in AFM micrographs.

186 CI does not block transcription. To ease the analysis and interpretation of the AFM images, nucleoprotein complexes were again categorized based on the position of RNAP along the DNA template in different experimental conditions. In control measurements, in the absence of 186 CI, we distinguished complexes where RNAP was found at the promoter from those where it had left it [Figure 3, left panel, top row]. The top row in the right panel of Figure 3 shows representative AFM images of these two categories.

In the presence of 186 CI, nucleoprotein complexes were found with the repressor bound to the pR/pL site only [Figure 3, right panel, middle row], or to both the pR/pL and FR sites [Figure 3, right panel, bottom row]. Therefore, we classified them according to the position of RNAP with respect to these two binding sites [Figure 3, left]. The images show that RNAP could be found in all regions. In a few cases (12%), 186 CI was found to be bound only at FR [Figure S4]. Note that nascent RNA is clearly visible associated with elongating RNAP in all images as highlighted in the zoomed areas at the top of the right panel of Figure 3.

The scoring of images, as described above, yielded the frequency histograms in Figure 2C. The red curve represents RNAP binding position in the absence of NTPs and 186 CI; the pink curve represents the surviving fraction of elongation complexes as a function of distance

from the promoter along the DNA molecule when NTPs were added in the absence of 186 CI. Before adding NTPs, 70% of the RNAP was found at the promoter, the rest was found between 100 and 500 bp. This may be due to the fact that the pR/pL site contains two promoters to which RNAP may also bind. After addition of NTPs, several rounds of transcription may take place on the same DNA template so that deposition on the mica for imaging captures nucleoprotein complexes and TECs at different stages of elongation. The blue and pink distributions in Figure 2C shows an exponential decay which ends at the terminator position (~1500 bp). The blue curve represents the surviving fraction of elongation complexes as a function of distance from the promoter along the DNA molecule in the presence of 186 CI and NTPs. We find that RNAP can elongate throughout the template. We also compared the binding position of 186 CI without and with RNAP. The green dash curve in Figure 2C shows that in the absence of RNAP, 186 CI was found to bind at pR/pL mainly and more rarely at FR. When RNAP and NTPs were added, 186 CI still bound predominantly at the pR/pL site, but in addition, the repressor was found at several other positions, as the orange bars of its position histogram show. These measurements indicate that 186 CI did not block elongation by RNAP and might in fact be pushed from pR/pL to non-specific sites.

Elongating RNA polymerase may cause the dissociation of 186 CI. We noted that in images like those in Figure 3, the size of 186 CI upstream of RNAP seemed smaller than most 186 CI found downstream of RNAP [Figure 3 right]. To test the idea that RNAP transcribing through the heptamer may cause the dissociation of some of its dimers from the wheel, we measured the diameter [Figure 4A] and volume [Figure 4B] of 186 CI under different conditions of transcription: (1) 100 nM 186 CI (no transcription control); (2) 500 nM 186 CI and RNAP without NTPs; (3) 500 nM 186 CI, RNAP and NTPs ; (4) 300 nM 186 CI, RNAP and NTPs; (5) 250 nM 186 CI, RNAP and NTPs. No obvious difference was detected between groups (1) and (2), which indicates that RNAP in the absence of transcription does not affect the size of 186 CI. Notice that the distribution of the diameter of 186 CI is wide under all experimental conditions, as previously reported[47]. Comparison of the diameter distributions of RNA polymerase and of 186 CI (without NTP) shows that the values of RNAP diameter are distributed more narrowly than those of 186 CI [Figure S5], which supports the idea that the broad distribution measured for 186 CI is not a technical artefact but is related to the 186 CI structure made out of the assembly of seven dimers. Group (3) represents transcription at the same 186 CI concentration used in measurement (2). There is a slight decrease in both diameter and volume of the 186 CI repressor. To verify that these differences were significant, we used the Welch's t-test to compare groups (2) and (3) and obtained t = 5.24, Df = 102, which means that the p value should be smaller than 0.0001, confirming that the difference is significant.

Decreasing the concentration of 186 CI from 550 nM to 300 nM and then to 250 nM in conditions of transcription, causes a further decrease of the diameter and volume of 186 CI. Taken together, these results point to the fact that: (i) elongating RNAP may cause at least the partial dissociation of 186 CI, otherwise the repressor diameter and volume would not decrease. (ii) The probability that 186 CI may rebind to the DNA template after dissociation depends on its concentration.

Figure 4 shows that the volume of 186 CI is largest, about 650 nm^3, in the absence of

transcription. This volume is consistent with what previously found for the full 186 CI wheel composed of seven dimers[46]. In the presence of transcription, the mean volume decreases, reaching its minimum, 255 nm^3, at the lowest 186 CI concentration used. This value is consistent with a structure containing 3 dimers, while the mean volume of ~420 nm^3 measured in TECs in the presence of 500 nM 186 CI, would represent 4 to 5 dimers.

Discussion

In order to compare the possible road-blocking activity of the λ and 186 CI repressors, their DNA-binding probability in different experimental conditions was plotted in Figure 5. There, the orange and green bars represent the percentage of repressor binding in the absence and presence of transcription, respectively. In the case of the λ CI repressor, in the absence of transcription, only 15 % of all DNA molecules imaged did not have any repressor bound to them. However, in the presence of transcription that percentage raised to 64 %. In addition, about 10 % of the DNA molecules with λ CI had only one operator region (either OL or OR) occupied, which is low compared to 75 % double λ CI complex binding (including unloop and looped DNA-λ CI complexes). After transcription, the percentage of DNA molecules with λ CI bound either at OL or at OR increased to 25 %, while the percentage of DNA molecules with both regions occupied by λ CI (unlooped and looped) decreased to 10 %. Before transcription, the percentage of DNA molecules looped by λ CI was 55 % while the unlooped nucleoprotein complexes were 20 %, but both decreased to 5 % after transcription [Figure 5A]. These decreases are consistent with the idea that λ CI dissociates from DNA when an RNAP elongates though it. On the other hand, the increase in the number of DNA molecules bound by only one λ CI oligomer indicates that some of the dislodged λ CI may rebind.

In the case of the 186 CI repressor, in the absence of transcription, nearly all DNA molecules were bound by repressor with only 2 % without it. In the presence of transcription, the percentage of DNA molecules without repressor increased to 32 %. On the other hand, before transcription, the percentage of repressor bound to either pR/pL or FR was 22 % and 6 %, respectively. This difference is likely due to the difference in affinity for the repressor of these two binding sites. In the presence of transcription, these percentages increase slightly to 32 % and 8 %, respectively. However, the percentage of DNA molecules with both pR/pL and FR bound by the 186 CI repressor is 70 % in the absence of transcription and only 28 % in the presence of transcription (Figure 5B).

Although the concentration of λ CI (150 nM) and 186 CI (500 nM) used in these measurements were quite different, we made a rough estimation of what the binding fraction of λ CI would be at 500 nM knowing that at [λ CI] = 150 nM its binding percentage is 85 % (see SI) [55]. We thus estimate it to be about 95 %. This means that 186 CI has similar binding affinity to DNA as λ CI. We also calculated that the free energy of binding of 186 CI dimer to DNA is ~ 19.6 k_BT [42] (see SI text), while free energy of binding of λ CI to the OR1 site is ~ 19.2 k_BT[56] (SI), in agreement with our result. Neither the unlooped DNA-λ CI nor the DNA-186 CI complex, interfere with RNAP elongation.

In our experiment, λ CI mediating a DNA loop blocked transcription efficiently. Although a

186 CI-mediated loop between pR and FR is possible[30, 45], it occurs with a very low probability in vitro[46] and it was never observed in the transcription measurements reported here.

The temperate λ and 186 bacteriophages are different, yet their CI repressors seem to have some structural similarities[57, 58]. Their N-terminal domain can bind to DNA, while the C-terminal domain interacts with that of a like dimer. Protein-protein cooperativity thus plays an important role in the regulatory function of these two repressors. Although the 186 CI repressor dimers oligomerize to form a wheel of seven units which preferentially wraps DNA at pR/pL, it can also, instead, bridge pR and FR inducing a DNA loop[45, 47]. The lack of such loops in AFM images of TECs seems to indicate that if formed, these loops are easily disrupted by elongating RNAPs.

Statistical analysis of the images indicates that the λ and 186 CI repressors tend to rebind to DNA after an RNAP has elongated past them. However, the data also indicate that 186 CI may rebind more easily than λ CI.

The possible mechanism by which RNAP may bypass each repressor is described in Figure 6. Figure 6A depicts the case of the λ CI repressor. When λ CI closes a DNA loop, RNAP is stalled at the loop entry; when the λ CI-mediated loop breaks down, RNAP causes the dissociation of the λ CI dimers from their operators and may also disrupt any oligomer they might have formed. After that, λ CI dimers can rebind DNA. Figure 6B depicts the possible interaction between 186 CI and RNAP. An elongating RNAP is likely to cause the dissociation of successive dimers in the wheel and when the three dimers bound to the highest affinity pR sites are dissociated, the whole wheel may dissociate and disaggregate. Based on the volumes of particles measured in Figure 4, the smallest particle likely to rebind will consist of 3 dimers, consistent with the three strong operators at 186 pR/pL, and could then interact with more dimers until the full 7-dimer wheel is reassembled. In conclusion, the present study shows that the λ CI and 186 CI repressors do not interfere significantly with transcription and suggests a mechanism by which they could regain their regulatory function on the DNA template.

Acknowledgments

This work was supported by the National Institutes of Health to L.F. (R01 GM084070) and Australian Research Council to KS (DP150103009). Kathleen Matthews at Rice University generously provided the LacI protein. We thank Ian Dodd for comments on the manuscript.

Bibliography

[1] Keenen, M. M., Brown, D., Brennan, L. D., Renger, R., Khoo, H., Carlson, C. R., Huang, B., Grill, S. W., Narlikar, G. J., and Redding, S. (2021) HP1 proteins compact DNA into mechanically and positionally stable phase separated domains, *eLife 10*, e64563.

[2] Syrjänen, J. L., Heller, I., Candelli, A., Davies, O. R., Peterman, E. J., Wuite, G. J., and Pellegrini, L. (2017) Single-molecule observation of DNA compaction by meiotic protein SYCP3, *eLife 6*.

[3] Hashimoto, T., and Kunieda, T. (2017) DNA Protection Protein, a Novel Mechanism of Radiation Tolerance: Lessons from Tardigrades, *Life 7,* 26.

[4] Sui, J., Zhang, S., and Chen, B. P. C. (2020) DNA–dependent protein kinase in telomere maintenance and protection, *Cellular & Molecular Biology Letters 25,* 2.

[5] McKinnon, P. J. (2016) Topoisomerases and the regulation of neural function, *Nature Reviews Neuroscience 17,* 673-679.

[6] Madabhushi, R. (2018) The Roles of DNA Topoisomerase IIβ in Transcription, *Int J Mol Sci 19*.

[7] Sobhy, H., Kumar, R., Lewerentz, J., Lizana, L., and Stenberg, P. (2019) Highly interacting regions of the human genome are enriched with enhancers and bound by DNA repair proteins, *Scientific reports 9,* 4577.

[8] Hammel, M., Rashid, I., Sverzhinsky, A., Pourfarjam, Y., Tsai, M.-S., Ellenberger, T., Pascal, J. M., Kim, I.-K., Tainer, J. A., and Tomkinson, A. E. (2020) An atypical BRCT–BRCT interaction with the XRCC1 scaffold protein compacts human DNA Ligase IIIα within a flexible DNA repair complex, *Nucleic Acids Research 49,* 306-321.

[9] Tse, E. C. M., Zwang, T. J., Bedoya, S., and Barton, J. K. (2019) Effective Distance for DNA-Mediated Charge Transport between Repair Proteins, *ACS Central Science 5,* 65-72.

[10] Maksimenko, O., and Georgiev, P. (2014) Mechanisms and proteins involved in long-distance interactions, *Front Genet 5,* 28-28.

[11] Kong, N., and Jung, I. (2020) Long-range chromatin interactions in pathogenic gene expression control, *Transcription 11,* 211-216.

[12] Hodges, C., Bintu, L., Lubkowska, L., Kashlev, M., and Bustamante, C. (2009) Nucleosomal fluctuations govern the transcription dynamics of RNA polymerase II, *Science 325,* 626-628.

[13] Bintu, L., Kopaczynska, M., Hodges, C., Lubkowska, L., Kashlev, M., and Bustamante, C. (2011) The elongation rate of RNA polymerase determines the fate of transcribed nucleosomes, *Nat Struct Mol Biol 18,* 1394-1399.

[14] Bintu, L., Ishibashi, T., Dangkulwanich, M., Wu, Y. Y., Lubkowska, L., Kashlev, M., and Bustamante, C. (2012) Nucleosomal Elements that Control the Topography of the Barrier to Transcription, *Cell 151,* 738-749.

[15] Jin, J., Bai, L., Johnson, D. S., Fulbright, R. M., Kireeva, M. L., Kashlev, M., and Wang, M. D. (2010) Synergistic action of RNA polymerases in overcoming the nucleosomal barrier, *Nat Struct Mol Biol 17,* 745-752.

[16] Zhang, T., Cooper, S., and Brockdorff, N. (2015) The interplay of histone modifications – writers that read, *EMBO reports 16,* 1467-1481.

[17] Xin, B., and Rohs, R. (2018) Relationship between histone modifications and transcription factor binding is protein family specific, *Genome Res 28,* 321-333.

[18] Smith, N. C., and Matthews, J. M. (2016) Mechanisms of DNA-binding specificity and functional gene regulation by transcription factors, *Current Opinion in Structural Biology 38,* 68-74.

[19] Grossman, S. R., Engreitz, J., Ray, J. P., Nguyen, T. H., Hacohen, N., and Lander, E. S. (2018) Positional specificity of different transcription factor classes within enhancers, *Proceedings of the National Academy of Sciences 115,* E7222.

[20] Long, Hannah K., Prescott, Sara L., and Wysocka, J. (2016) Ever-Changing Landscapes: Transcriptional Enhancers in Development and Evolution, *Cell 167,* 1170-1187.

[21] Mendes, M. A., Guerra, R. F., Berns, M. C., Manzo, C., Masiero, S., Finzi, L., Kater, M. M., and Colombo, L. (2013) MADS Domain Transcription Factors Mediate Short-Range DNA Looping That Is Essential for Target Gene Expression in Arabidopsis, *The Plant Cell 25,* 2560-2572.

[22] Garcia, H. G., and Phillips, R. (2011) Quantitative dissection of the simple repression input-output function, *Proc Natl Acad Sci U S A 108*, 12173-12178.

[23] Vörös, Z., Yan, Y., Kovari, D. T., Finzi, L., and Dunlap, D. (2017) Proteins mediating DNA loops effectively block transcription, *Protein Science 26*, 1427-1438.

[24] Xu, W., Yan, Y., Artsimovitch, I., Sunday, N., Dunlap, D., and Finzi, L. (2021) Transcription elongation through lac repressor-mediated DNA loops, *bioRxiv*, 2021.2003.2002.433568.

[25] Lewis, M. (2005) The lac repressor, *Comptes Rendus Biologies 328*, 521-548.

[26] Finzi, L., and Gelles, J. (1995) Measurement of lactose repressor-mediated loop formation and breakdown in single DNA molecules, *Science 267*, 378-380.

[27] Cournac, A., and Plumbridge, J. (2013) DNA Looping in Prokaryotes: Experimental and Theoretical Approaches, *Journal of Bacteriology 195*, 1109-1119.

[28] Hao, N., Sullivan, A. E., Shearwin, K. E., and Dodd, I. B. (2021) The loopometer: a quantitative in vivo assay for DNA-looping proteins, *Nucleic Acids Research 49*, e39-e39.

[29] Ptashne, M. (2004) *A genetic Switch: Phage Lambda Revisited*, 3rd ed., Cold Spring Harbor Laboratory Press.

[30] Pinkett, H. W., Shearwin, K. E., Stayrook, S., Dodd, I. B., Burr, T., Hochschild, A., Egan, J. B., and Lewis, M. (2006) The structural basis of cooperative regulation at an alternate genetic switch, *Mol Cell 21*, 605-615.

[31] Atsumi, S., and Little, J. W. (2006) Role of the lytic repressor in prophage induction of phage lambda as analyzed by a module-replacement approach, *Proceedings of the National Academy of Sciences of the United States of America 103*, 4558-4563.

[32] Little, J. W., Shepley, D. P., and Wert, D. W. (1999) Robustness of a gene regulatory circuit, *Embo Journal 18*, 4299-4307.

[33] Kim, Y. I., and Hu, J. C. (1995) Operator binding by lambda repressor heterodimers with one or two N-terminal arms, *Proceedings of the National Academy of Sciences of the United States of America 92*, 7510-7514.

[34] Sarkar-Banerjee, S., Goyal, S., Gao, N., Mack, J., Thompson, B., Dunlap, D., Chattopadhyay, K., and Finzi, L. (2018) Specifically bound lambda repressor dimers promote adjacent non-specific binding, *PLoS One 13*, e0194930.

[35] Stayrook, S., Jaru-Ampornpan, P., Ni, J., Hochschild, A., Lewis, M.,. (2008) Crystal structure of the lambda repressor and a model for pairwise cooperative operator binding, *Nature 452*, 1022-1026.

[36] Michalowski, C. B., and Little, J. W. (2013) Role of cis-Acting Sites in Stimulation of the Phage λ PRM Promoter by CI-Mediated Looping, *Journal of Bacteriology 195*, 3401-3411.

[37] Zurla, C., Manzo, C., Dunlap, D., Lewis, D. E. A., Adhya, S., and Finzi, L. (2009) Direct demonstration and quantification of long-range DNA looping by the λ bacteriophage repressor, *Nucleic Acids Research 37*, 2789-2795.

[38] Anderson, L. M., and Yang, H. (2008) DNA looping can enhance lysogenic CI transcription in phage lambda, *Proceedings of the National Academy of Sciences of the United States of America 105*, 5827-5832.

[39] Lewis, D., Le, P., Zurla, C., Finzi, L., and Adhya, S. (2011) Multilevel autoregulation of lambda repressor protein CI by DNA looping in vitro, *Proceedings of The National Academy of Sciences of The United States of America 108*, 14807-14812.

[40] Dodd, I. B., Perkins, A. J., Tsemitsidis, D., and Egan, J. B. (2001) Octamerization of lambda CI repressor is needed for effective repression of P-RM and efficient switching from lysogeny, *Genes & Development 15*, 3013-3022.

[41] Dodd, I. B., Shearwin, K. E., Perkins, A. J., Burr, T., Hochschild, A., and Egan, J. B. (2004) Cooperativity in long-range gene regulation by the lambda CI repressor, *Genes & Development 18*, 344-354.

[42] Dodd, I. B., and Egan, J. B. (1996) DNA binding by the coliphage 186 repressor protein CI, *Journal Of Biological Chemistry 271*, 11532-11540.

[43] Dodd, I. B., and Egan, J. B. (2002) Action at a distance in CI repressor regulation of the bacteriophage 186 genetic switch, *Molecular Microbiology 45*, 697-710.

[44] Egan, K. E. S. a. J. B. (1996) Purification and self-association equilibria of the lysis-lysogeny switch proteins of coliphage 186, *The Journal of Biological Chemistry 271*, 7.

[45] Dodd, I. B., Shearwin, K. B., and Sneppen, K. (2007) Modelling transcriptional interference and DNA looping in gene regulation, *Journal Of Molecular Biology 369*, 1200-1213.

[46] Wang, H. W., Dodd, I. B., Dunlap, D. D., Shearwin, K. E., and Finzi, L. (2013) Single molecule analysis of DNA wrapping and looping by a circular 14mer wheel of the bacteriophage 186 CI repressor, *Nucleic Acids Research 41*, 5746-5756.

[47] Wang, H., Dodd, I. B., Dunlap, D. D., Shearwin, K. E., and Finzi, L. (2013) Single molecule analysis of DNA wrapping and looping by a circular 14mer wheel of the bacteriophage 186 CI repressor, *Nucleic Acids Res 41*, 5746-5756.

[48] Chong, S., Chen, C., Ge, H., and Xie, X. S. (2014) Mechanism of transcriptional bursting in bacteria, *Cell 158*.

[49] Le, T. B. K., Imakaev, M. V., Mirny, L. A., and Laub, M. T. (2013) High-resolution mapping of the spatial organization of a bacterial chromosome, *Science (New York, N.Y.) 342*, 731-734.

[50] Naughton, C., Avlonitis, N., Corless, S., Prendergast, J. G., Mati, I. K., Eijk, P. P., Cockroft, S. L., Bradley, M., Ylstra, B., and Gilbert, N. (2013) Transcription forms and remodels supercoiling domains unfolding large-scale chromatin structures, *Nat Struct Mol Biol 20*, 387-395.

[51] Wang, H., Finzi, L., Lewis, D. E., and Dunlap, D. (2009) AFM studies of lambda repressor oligomers securing DNA loops, *Curr Pharm Biotechnol 10*, 494-501.

[52] Meyer, B. J., Maurer, R., and Ptashne, M. (1980) Gene regulation at the right operator (OR) of bacteriophage lambda. II. OR1, OR2, and OR3: their roles in mediating the effects of repressor and cro, *J Mol Biol 139*, 163-194.

[53] Meyer, B. J., and Ptashne, M. (1980) Gene regulation at the right operator (OR) of bacteriophage lambda. III. lambda repressor directly activates gene transcription, *J Mol Biol 139*, 195-205.

[54] Dodd, I. B., Shearwin, K. E., and Egan, J. B. (2005) Revisited gene regulation in bacteriophage lambda, *Current Opinion In Genetics & Development 15*, 145-152.

[55] Yang, Y., Sass, L. E., Du, C., Hsieh, P., and Erie, D. A. (2005) Determination of protein-DNA binding constants and specificities from statistical analyses of single molecules: MutS-DNA interactions, *Nucleic Acids Res 33*, 4322-4334.

[56] Merabet, E., and Ackers, G. K. (1995) Calorimetric analysis of lambda cI repressor binding to DNA operator sites, *Biochemistry 34*, 8554-8563.

[57] Dodd, I. B., and Egan, J. B. (1988) The Prediction Of Helix-Turn-Helix Dna-Binding Regions In Proteins - A Reply, *Protein Engineering 2*, 174-175.

[58] Shearwin, K. E., Dodd, I. B., and Egan, J. B. (2002) The helix-turn-helix motif of the coliphage 186 immunity repressor binds to two distinct recognition sequences, *Journal Of Biological Chemistry 277*, 3186-3194.

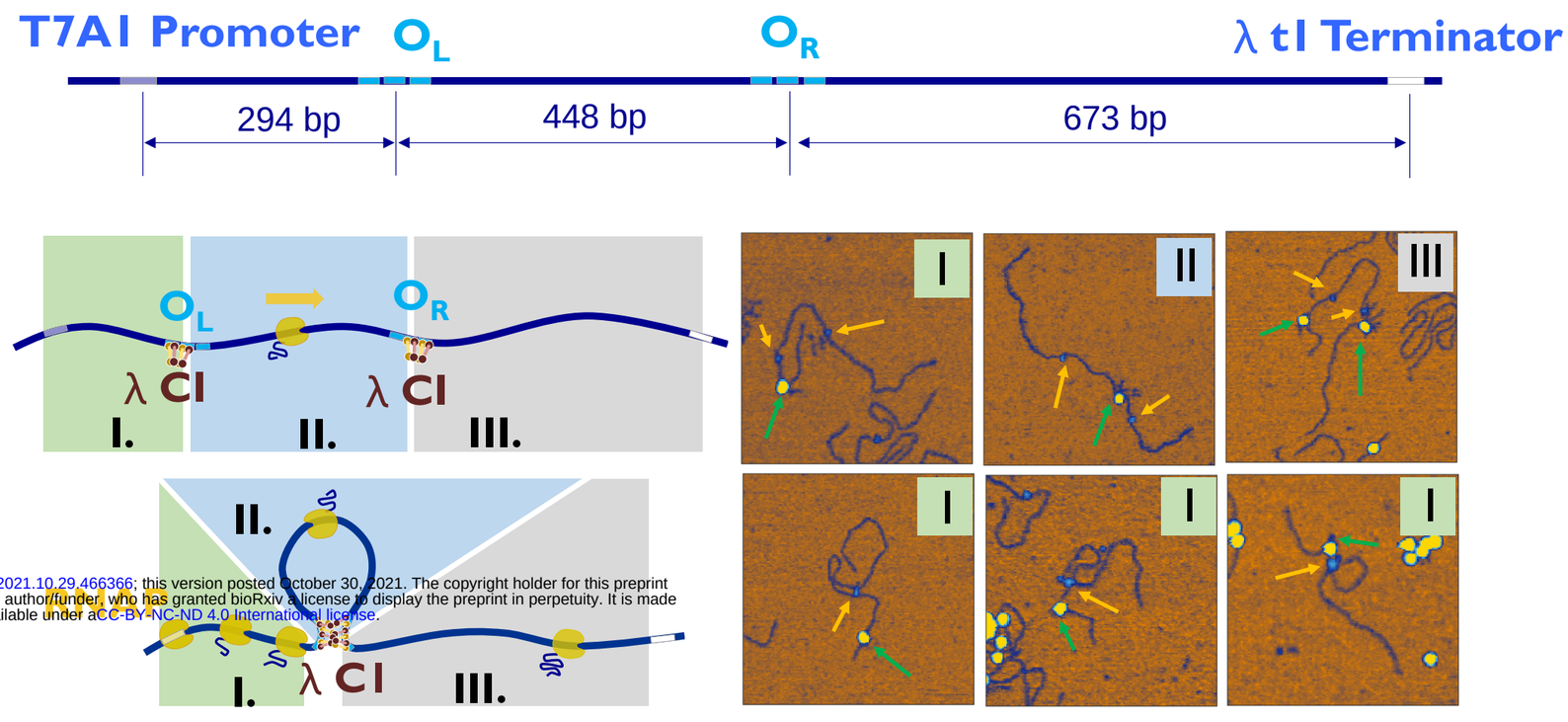

Figure 1. RNAP elongation in the presence of λ CI repressor. (Top) Diagram of DNA template used. (Bottom Left) Cartoons describing the different regions where RNAP may be found with respect to the repressor bound to its operators. (Bottom Right) Gallery of transcription elongation complexes along a DNA template containing the OL and OR λ operators in the presence of the λ CI repressor. RNAP is yellow, DNA blue and λ CI cyan. The top right AFM image shows that a second RNAP had started elongation of the same DNA template, while a first RNAP had just bypassed λ CI bound at the OR region. No looped molecules were found with RNAP inside or after the loop.

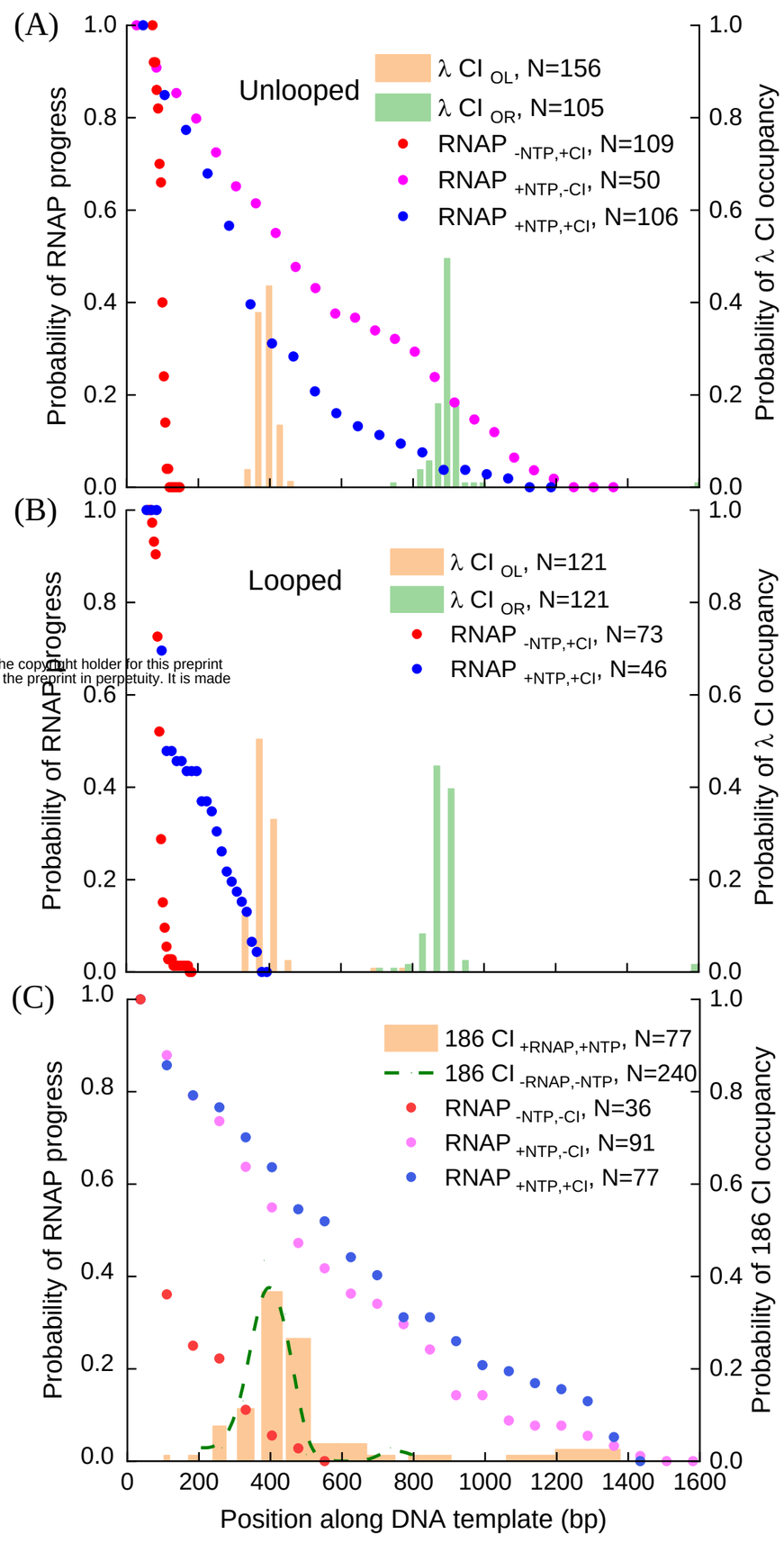

Figure 2. Comparison of RNAP progress in the presence of either the λ or 186 CI repressor. The orange and green histograms indicate the location of bound proteins; the colors dots indicate the surviving fraction of elongation complexes as a function of distance from the promoter along the DNA molecule. (A-B) Elongation on unlooped and looped DNA templates, respectively, in the presence of λ CI. (C) Elongation in the presence of 186 CI.

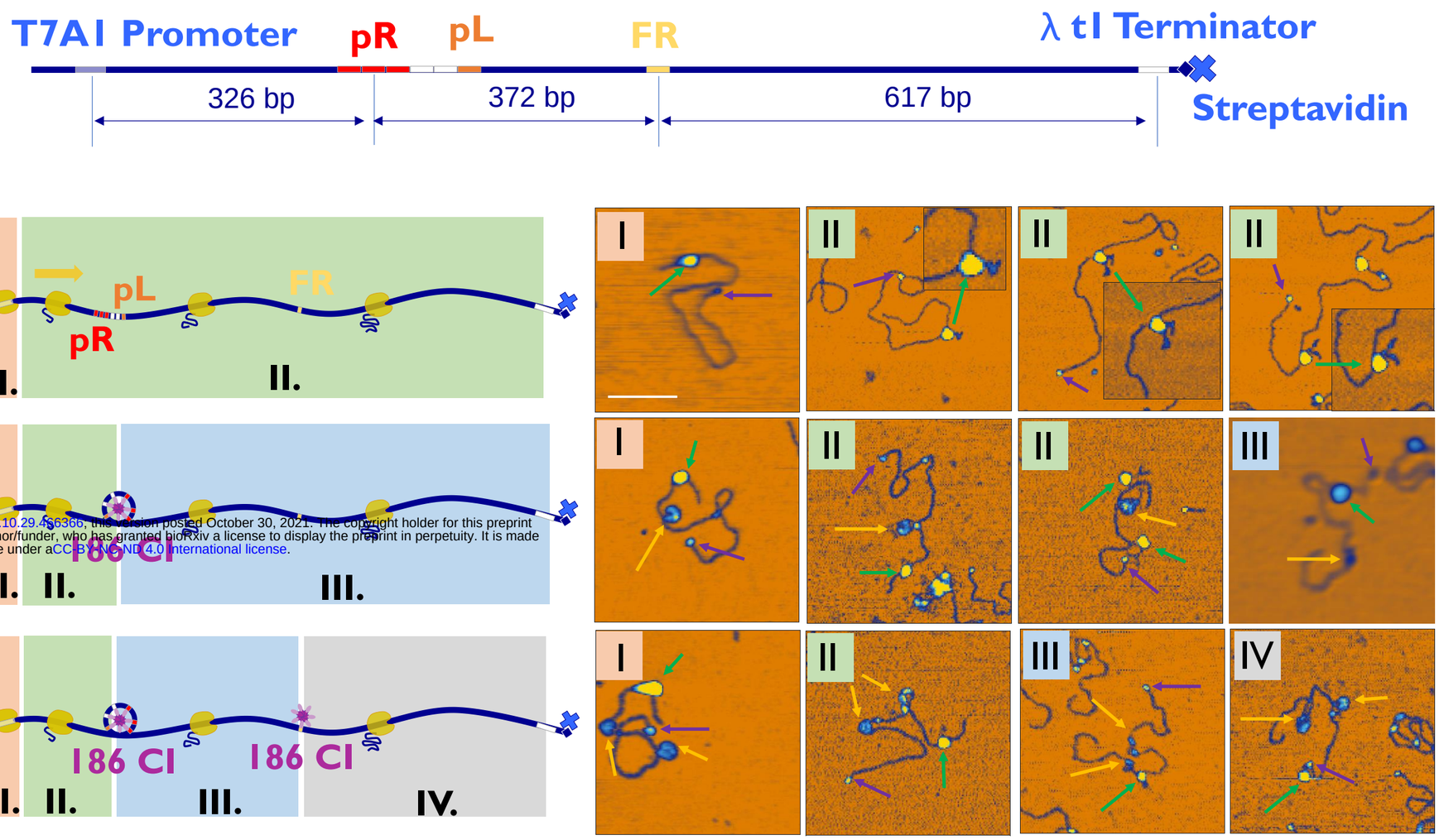

Figure 3. RNAP elongation in the presence of the 186 CI repressor. (Top) Diagram of DNA template used. (Bottom Left) Cartoons describing the different regions where RNAP may be found with respect to the repressor bound to its operators. (Bottom Right) Gallery of transcription elongation complexes along a DNA template in the presence of the 186 CI repressor color-coded according to the cartoons at left.

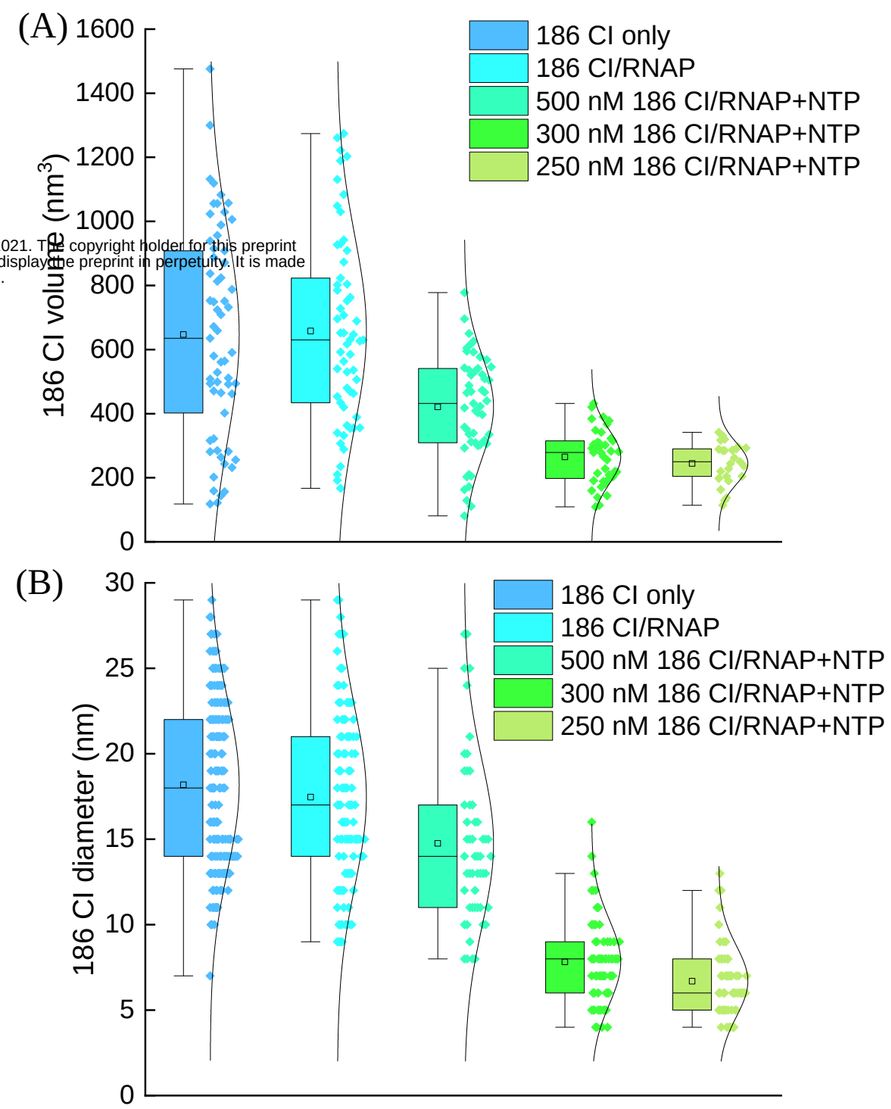

Figure 4. The 186 CI heptameric wheel is disrupted by RNAP elongation. Whisker and violin plots of the 186 diameter (A) and volume (B) measured in AFM transcription assays. The conditions from left to right are: 150 nM 186 CI only; 500 nM 186 CI/RNAP only; 500 nM 186 CI/RNAP+NTP; 300 nM 186 CI/RNAP+NTP; 250 nM 186 CI/RNAP+NTP。

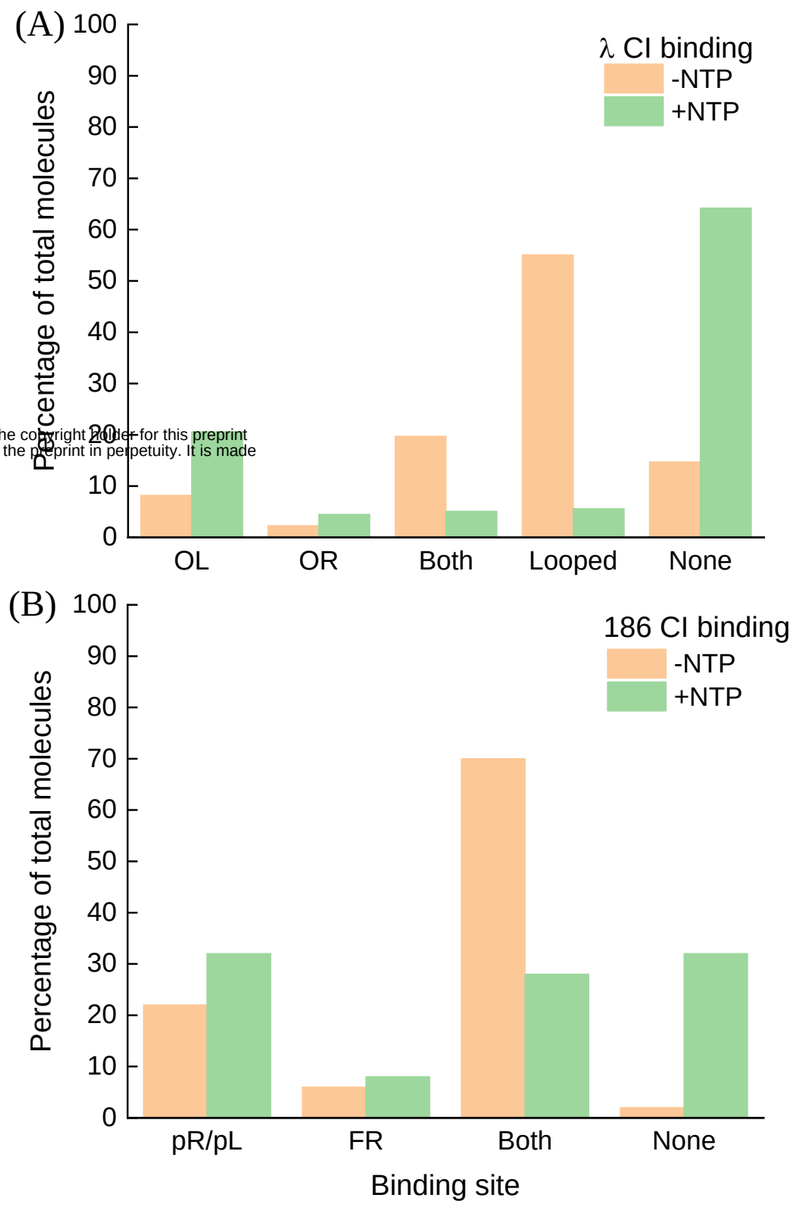

Figure 5. λ and 186 repressors do not seem to be strong roadblocks. λ CI (A) and 186 (B) CI binding distribution before and after transcription.

Proposed mechanism of transcription progress with a CI obstacle

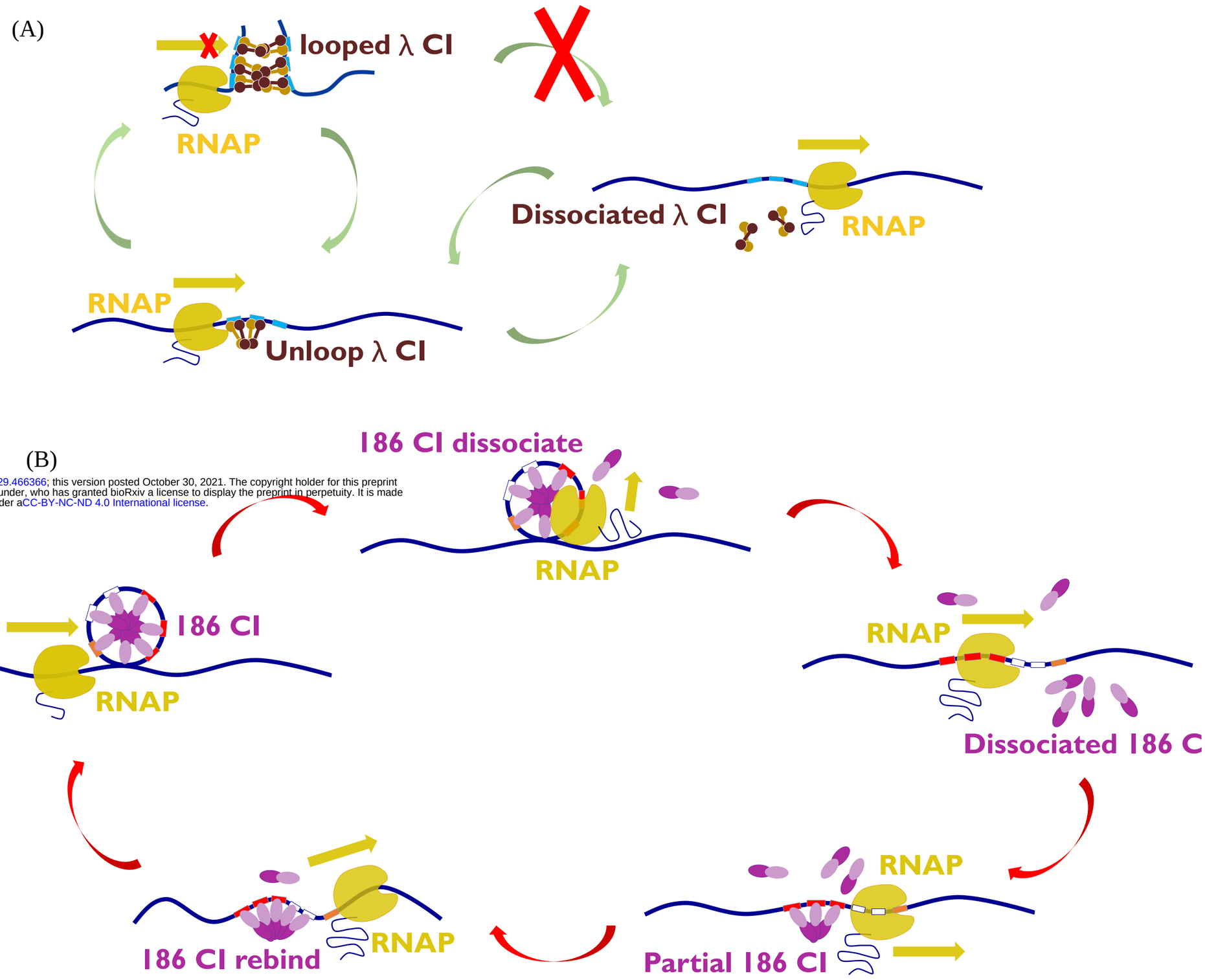

Figure 6. Schematic of RNA polymerase transcript bypass the λ CI (A) and 186 CI (B).
For λ CI, if loop complex form, RNA polymerase cannot bypass it. However, loop and unloop complex can transform. When unloop complex form, RNA polymerase will transcript bypass the obstacle and may dissociate λ CI.
For 186 CI, RNA polymerase can bypass the complex and dissociate the wheel-like structure, but 186 CI may rebind and then form the wheel-like structure.